QuikSCAT Wind Retrievals for Tropical Cyclones

Simon H. Yueh, *Senior Member, IEEE*, Bryan W. Stiles, and W. Timothy Liu

***Abstract*—The use of QuikSCAT data for wind retrievals of tropical cyclones is described. The evidence of QuikSCAT σ_0 dependence on wind direction for >30-m/s wind speeds is presented. The QuikSCAT $\sigma_0 s$ show a peak-to-peak wind direction modulation of ~1 dB at 35-m/s wind speed, and the amplitude of modulation decreases with increasing wind speed. The decreasing directional sensitivity to wind speed agrees well with the trend of QSCAT1 model function at near 20 m/s. A correction of the QSCAT1 model function for above 23-m/s wind speed is proposed. We explored two microwave radiative transfer models to correct the attenuation and scattering effects of rain for wind retrievals. One is derived from the collocated QuikSCAT and Special Sensor Microwave/Imager (SSM/I) dataset, and the other one is a published parametric model developed for rain radars. These two radiative transfer models account for the effects of volume scattering, scattering from rain-roughened surfaces and rain attenuation. The models suggest that the $\sigma_0 s$ of wind-roughened sea surfaces for 40–50-m/s winds are comparable to the $\sigma_0 s$ of rain contributions for up to about 10–15 mm/h. Both radiative transfer models have been used to retrieve the ocean wind vectors from the collocated QuikSCAT and SSM/I rain rate data for several tropical cyclones. The resulting wind speed estimates of these tropical cyclones show improved agreement with the wind fields derived from the best track analysis and Holland's model for up to about 15-mm/h SSM/I rain rate. A comparative analysis of maximum wind speed estimates suggests that other rain parameters likely have to be considered for further improvements.**

***Index Terms*—Hurricane, ocean wind, rain attenuation, rain scattering, scatterometer, tropical cyclone.**

I. Introduction

SKILLFUL FORECASTS of tropical cyclone (TC) track and intensity depend on an accurate depiction of the initial conditions of air and sea states in TC forecast models [1]. A primary source of difficulty in past efforts for TC forecasts has been the inability to make direct observations of the surface wind field, which is one of the key driving forces for the heat and moisture exchanges between the air and sea surfaces [2]–[4]. There are strong needs for global high-wind observations from satellites [5].

QuikSCAT, which is the SeaWinds scatterometer on the QuikSCAT satellite, is a spaceborne Ku-band (13.402 GHz) scatterometer designed to measure the normalized radar cross section (σ_0) of sea surfaces. The ocean surface σ_0 at Ku-band is sensitive to the ocean surface wind velocity (speed and direction). The relationship between $\sigma_0 s$ and the ocean surface wind velocity, usually described by a geophysical model function (GMF), enables the retrieval of ocean surface winds from scatterometer measurements.

QuikSCAT uses a conical scanning antenna reflector, illuminated by two antenna feed horns to produce two antenna beams (Fig. 1). The inner beam operates at a nominal incidence angle of 46° with horizontal polarization and the outer beam operates at a nominal 54° incidence angle with vertical polarization. During a satellite pass, a wind vector cell (WVC) will be observed at fore- and aft-looking azimuth directions by the antenna. The dimension of QuikSCAT WVC is 25 km across track and 25 km along track. The relative azimuth angle between the fore- and aft-looks varies between 0° to 180°, depending on where the WVC is located within the swath. This azimuth diversity enables the investigation of the wind direction dependence of $\sigma_0 s$ for TCs.

The QuikSCAT scatterometer has been operating since August 1999 to provide global mapping of ocean winds. It was shown to be accurate for wind speed of up to at least 20 m/s [6]. The global wind fields from QuikSCAT have been routinely assimilated into the numerical weather prediction systems operated by the National Center for Environmental Prediction (NCEP) and European Center for Medium-Range Weather Forecasts (ECMWF).

The performance of QuikSCAT is uncertain for above 20-m/s wind speeds. The development of the GMF and retrieval algorithm using spaceborne scatterometers for hurricane wind velocities is still under active research [7]–[12]. Published techniques for correcting the underestimates of satellite winds at high wind speeds include the use of surface pressure analysis [7] or a tuning of the GMF [8], [10], [12].

Numerous aircraft scatterometer campaigns over TCs have been performed to assess the scatterometer GMF for extreme high winds. The University of Massachusetts (UMASS) Ku-band scatterometer observations at vertical polarization demonstrated that there were wind speed signals in ocean $\sigma_0 s$ of TCs, although with a reduced sensitivity in comparison with lighter wind conditions (<20 m/s) [9], [10]. The dual-polarized observations made by the Jet Propulsion Laboratory (JPL) indicated that the Ku-band radar signature is polarized for hurricane wind conditions with the horizontal polarization being more responsive to the wind speed than the vertical polarization [11].

An examination of the QuikSCAT $\sigma_0 s$ of several Pacific and Atlantic TCs in 1999 confirmed the reduced wind speed sensitivity and polarized scattering behavior indicated by aircraft observations [12]. In addition, it was suggested that the wind speed sensitivity of $\sigma_0 s$ could extend beyond 40 m/s. However, the limited amount of data did not allow a more detailed analysis of wind direction dependence and rain effects.

Manuscript received January 5, 2003; revised April 28, 2003. The work carried out in this paper was performed by the Jet Propulsion Laboratory under contract with the National Aeronautics and Space Administration (NASA). This work was supported by the NASA research fund for the Ocean Vector Wind Science Team.

The authors are with the Jet Propulsion Laboratory, California Institute of Technology, Pasadena, CA 91109 USA (e-mail: simon.yueh@jpl.nasa.gov).

Digital Object Identifier 10.1109/TGRS.2003.814913

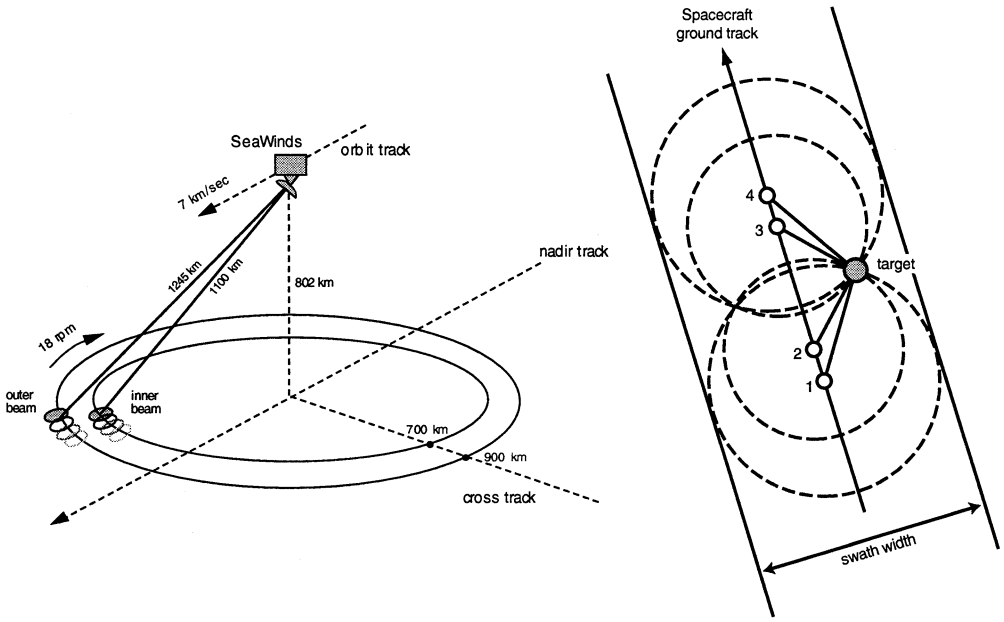

Fig. 1. Scanning geometry of the Seawinds scatterometer on the QuikSCAT spacecraft. Two antenna beams enable the sampling a wind vector cell from up to four different azimuth directions.

This paper presents the results from the analysis of QuiksCAT data from the 1999 and 2000 hurricane seasons for the wind direction modeling of ocean $\sigma_0 s$ for extreme high winds. A simple functional correction of the QSCAT1 GMF, presently used by the JPL and National Oceanic and Atmospheric Administration (NOAA) data processing systems for QuikSCAT, is proposed for rain-free conditions. We examined two radiative transfer (RT) models for the effects of rain. The coefficients of the RT models were taken from previously published research. The RT models present a physical picture regarding the relative significance of rain attenuation, volume scattering, and rain-drop-induced surface scattering. The RT models, together with the modified QuikSCAT GMF, were applied to the processing of QuikSCAT data to indicate how accurate the effects of rain can be corrected.

Section II discusses the effects of wind direction on QuikSCAT $\sigma_0 s$ of TCs and presents a correction model for the QSCAT1 GMF. Section III describes two radiative transfer models. Section IV illustrates and discusses the results from the application of the RT models for TC wind retrieval. Summary of our investigation is presented in Section V.

II. QUIKSCAT σ_0 OBSERVATIONS

The azimuth diversity of QuikSCAT fore- and aft-look geometry allows a direct examination of the wind direction dependence of TC $\sigma_0 s$. Fig. 2(a) and (b) illustrates the fore- and aft-look $\sigma_0 s$ acquired by the inner and outer antenna beams for hurricane Alberto in 2000. Alberto was considered to be the third-longest-lived tropical cyclone of record in the Atlantic and offered many QuikSCAT observations throughout its lifetime. The images, organized in five columns, illustrate the data from five QuikSCAT passes, including revs 5975, 5982, 5989, 5996, and 6103. Table I summarizes the best track intensities of Alberto from the National Hurricane Center (NHC) for these five QuikSCAT passes with the maximum wind speeds in the range of 44–56 m/s.

The σ_0 images in the first two rows of Fig. 2(a) and (b) indicate the evolution and location of Alberto. The spatial patterns of σ_0 appeared asymmetric with respect to the center of the cyclone, marked by black crosses. The locations of black crosses are based on a linear interpolation of the best track locations reported at certain times to the time of QuikSCAT observations. The interpolated eye locations appear reasonable for revs 5975 and 5982, but seem to be off by one to two QuikSCAT WVCs for revs 5996 and 6103 from the location of minimum σ_0 (purple color in Fig. 2) adjacent to the crosses. The location of minimum QuikSCAT $\sigma_0 s$ should be a more accurate indicator of the eye location, where lighter winds provide a lower radar scattering than the winds on the eye wall.

The images in the third row of Fig. 2(a) and (b) illustrate the σ_0 asymmetry (fore-look σ_0 divided by aft-look σ_0) in decibels between fore- and aft-look measurements. The σ_0 asymmetries, strikingly similar between inner and outer antenna beams, suggest the influence of wind direction on $\sigma_0 s$ for hurricane winds.

The effects of rain are indicated by a comparison of Fig. 2(c) with Fig. 2(a) and (b). The images in the first row of Fig. 2(c) correspond to the collocated rain rate from the Special Sensor Microwave Imager (SSM/I) [14]. Many parts of the cyclones had an SSM/I rain rate of lower than 10–15 mm/h. It should be noted that there is usually a time difference between the SSM/I and QuikSCAT passes, which can result in a spatial mismatch between SSM/I and QuikSCAT observations. For example, a cyclone with a forward motion of 10 m/s could travel 24 km in 40 min, comparable to the size of QuikSCAT WVC (25 km). Therefore, the brightness temperatures derived from the QuikSCAT receiver-noise-only measurements [13] are included in the second row of Fig. 2(c) to corroborate the spatial distribution of rain rate in the SSM/I images. The high SSM/I rain rates (orange color) typically correspond to high QuikSCAT

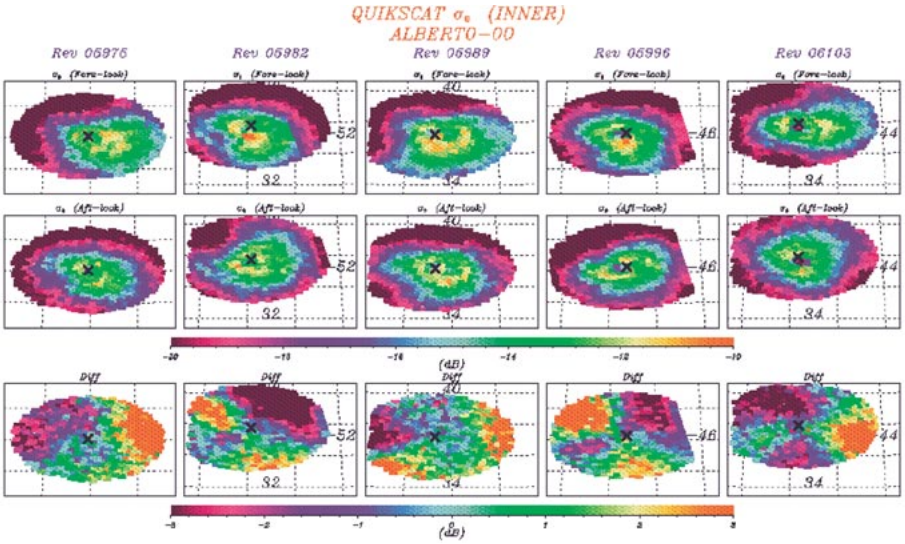

(a)

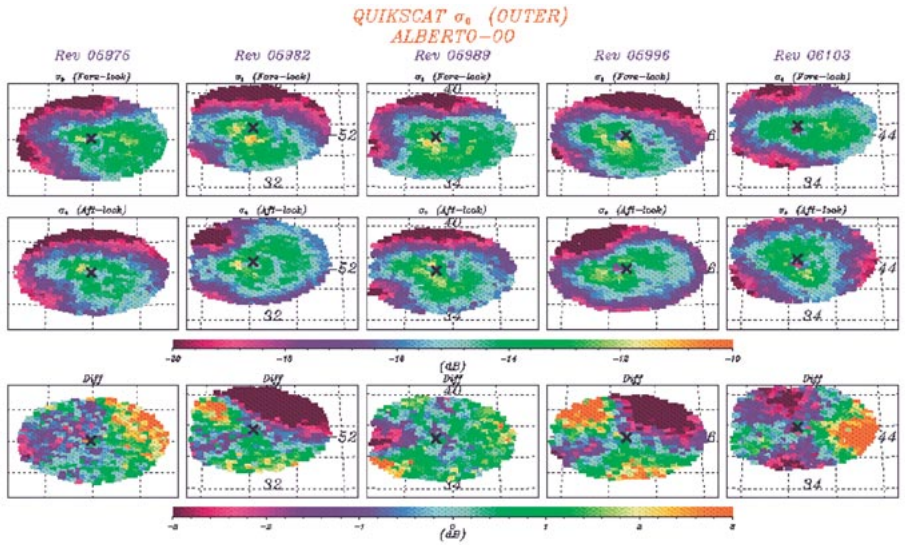

(b)

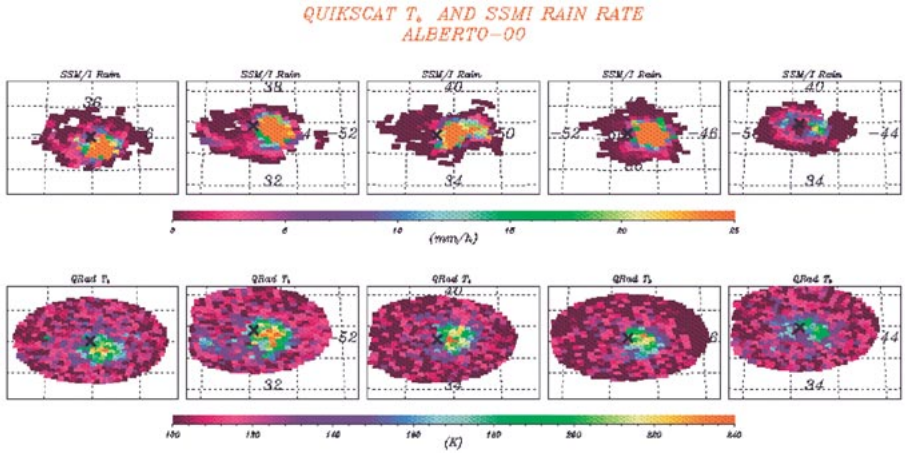

(c)

Fig. 2. (a) Images of QuikSCAT inner beam $\sigma_0 s$ with the first row for the fore-look observations, the second row for aft-look observations, and the third row for the ratio of fore- and aft-look data. (b) Outer beam $\sigma_0 s$. (c) SSM/I rain rate (first row) and QuikSCAT brightness temperature (second row) for hurricane Alberto in August 2000. Five revs of data are organized in five columns.

brightness temperatures (red-green color). An examination of the images in Fig. 2(a)–(c) indicates that the regions of high rain rate (>20 mm/h) have lower $\sigma_0 s$ than the neighboring areas, indicative of the attenuation effects of rain.

TABLE I
KEY CHARACTERISTICS OF HURRICANE ALBERTO FOR FIVE QUIKSCAT PASSES. THE VELOCITY OF FORWARD MOTION AND MAXIMUM WIND SPEED WERE DERIVED FROM THE NHC BEST TRACK ANALYSIS. THE DIRECTION OF MOTION IS DEFINED AS THE ANGLE IN CLOCKWISE DIRECTION FROM THE NORTH. THE TIME DIFFERENCE BETWEEN THE QUIKSCAT AND THE CLOSEST SSM/I PASS IN TIME IS DESCRIBED IN COLUMN 5

QuikSCAT Rev	Maximum Wind Speed (m/s)	TC forward motion Speed (m/s) ∠ Direction (deg.)	Date/time of QuikSCAT satellite pass (UT)	Time difference between QuikSCAT and SSM/I passes (min)
5975	47	8.6∠33	8/11/2000, 22:15	40
5982	52	8∠55	8/12/2000, 9:31	40
5989	56	9∠66	8/12/2000, 21:49	18
5996	46	8∠75	8/13/2000, 9:06	48
6103	44	1.6∠50	8/20/2000, 9:47	150

It is shown in Fig. 2 that there are differing $\sigma_0 s$ between fore- and aft-look observations. Fig. 3 illustrates the $\sigma_0 s$ taken from two cuts through the eye of the hurricane for rev 5989. The rain rate was mostly less than 10 mm/h on the along-track cut, where there is wetter atmosphere on the north side of the eye. To the south of the eye, there is about 0.5–1-dB difference between the fore- and aft-look observations. The difference increases with increasing distance from the eye and reaches as large as 3 dB for the inner beam (horizontal polarization) and 2 dB for the outer beam (vertical polarization) at about 200 km off the eye. It is not expected that the scattering and attenuation effects of rain will introduce significant difference between fore and aft-look measurements. The results imply that the directional dependence of $\sigma_0 s$ decreases with increasing wind speed (approaching the eye), but may still have a directional dependence of about 0.5 dB at 40–50-m/s wind speeds.

Fig. 3 also indicates the effects of rain on the $\sigma_0 s$ near the eye, where extreme high wind is expected. The data bounded by two vertical dash lines in the across-track panels correspond to high SSM/I rain rate and QuikSCAT brightness temperatures. Rain appeared to make the $\sigma_0 s$ in this region lower than that of the adjacent areas. Examination of several other revs of QuikSCAT data indicates similar characteristics.

The wind direction dependence of $\sigma_0 s$ can be expressed in terms of a cosine series with coefficient A_i denoting the amplitude of the ith harmonics. Using the ratios of fore- and aft-look σ_0 observations, we estimated the upwind and crosswind asymmetry of $\sigma_0 s$ by neglecting the upwind and downwind asymmetry. Specifically, we made the approximation for extreme high wind: $\sigma_0 = A_0 + A_2 \cos(2\phi)$, where ϕ is the relative angle between the wind and antenna look directions. Following the procedure described in [12] using the Holland model for hurricane winds [19] to provide the wind speed and direction, we estimated the ratio A_2/A_0 from the ratio (r) of each pair of fore- and aft-look $\sigma_0 s$

$$\frac{A_2}{A_0} = \frac{r-1}{\cos(\phi_W - \phi_F) - r\cos(\phi_W - \phi_A)}. \tag{1}$$

Here ϕ_W, ϕ_F, and ϕ_A represent the directions of wind, fore look, and aft look, respectively. Explicitly, $r = \sigma_{0,\mathrm{fore}}/\sigma_{0,\mathrm{aft}}$ with $\sigma_{0,\mathrm{fore}}$ and $\sigma_{0,\mathrm{aft}}$ denoting the $\sigma_0 s$ from fore- and aft-looks, respectively. The estimate of A_2/A_0 is performed only if the denominator on the right-hand side of the equation is greater than 0.5.

The estimates were binned and averaged as a function of wind speed and rain rate using data from the QuikSCAT passes of hurricanes in 1999 and 2000. The estimates of A_2/A_0 ratios are illustrated against the QSCAT1 and NSCAT2 GMFs [15] in the two lower panels of Fig. 4. The A_2/A_0 ratios from the QSCAT1 and NSCAT2 GMFs are constant at about 1 dB for above 23-m/s wind speed. The constant values were assumptions because there is a lack of accurate high wind speed predictions in the numerical weather analyses for developing the QSCAT1 and NSCAT2 GMFs. Our estimates of A_2/A_0 ratios for 0–2- and 2–4-mm/h rain bins follow well with the decreasing trend of QSCAT1 and NSCAT2 A_2/A_0 ratios at near 20-m/s wind speeds.

To reach a better agreement with the QuikSCAT estimates, we propose the following modifications to the QSCAT1 GMF for wind speeds (w) above $w_C = 23$ m/s:

$$\frac{A_i}{A_0} = \frac{1 - \exp\left[-\left(\frac{25}{w}\right)^2\right]}{1 - \exp\left[-\left(\frac{25}{w_C}\right)^2\right]} \frac{A_i}{A_{0\,\mathrm{QSCAT1},w=w_C}} \tag{2}$$

for $i \geq 1$ and

$$A_0 = A_{0,\mathrm{QSCAT1}}(w_C) + \beta(w - w_C). \tag{3}$$

Here w is the wind speed in meters per second. The value of β is 0.0025 for inner beam and 0.0018 for outer beam [12]. The modified GMF is illustrated in Fig. 4 with legend QSTC02. The empirical correction makes the modified GMF in closer agreement with the data.

III. RADIATIVE TRANSFER MODELING

Rain will attenuate the radar signal, introduce volume scattering from raindrops, and roughen water surfaces to produce surface scattering. To account for the effects of rain, we assume the following radiative transfer model for QuikSCAT observations:

$$\sigma_0 = \sigma_{0\mathrm{RV}} + \exp\left(-\frac{2kH}{\cos\theta}\right)(\sigma_{0\mathrm{WIND}} + \sigma_{0\mathrm{RS}}). \tag{4}$$

Here $\sigma_{0\mathrm{RV}}$ represents the integrated volume scattering from raindrops with attenuation by the rain layer above the raindrops. The attenuation per unit length is denoted by k. $\sigma_{0\mathrm{RS}}$ corresponds to the scattering from the surface roughness due to rain impact. $\sigma_{0\mathrm{WIND}}$ is the QuikSCAT GMF for rain-free conditions. This model neglects the interaction between wind waves and rain impact.

The above model assumes a stratified rain layer with constant rain rate R and column height of H. For this model, the two-way

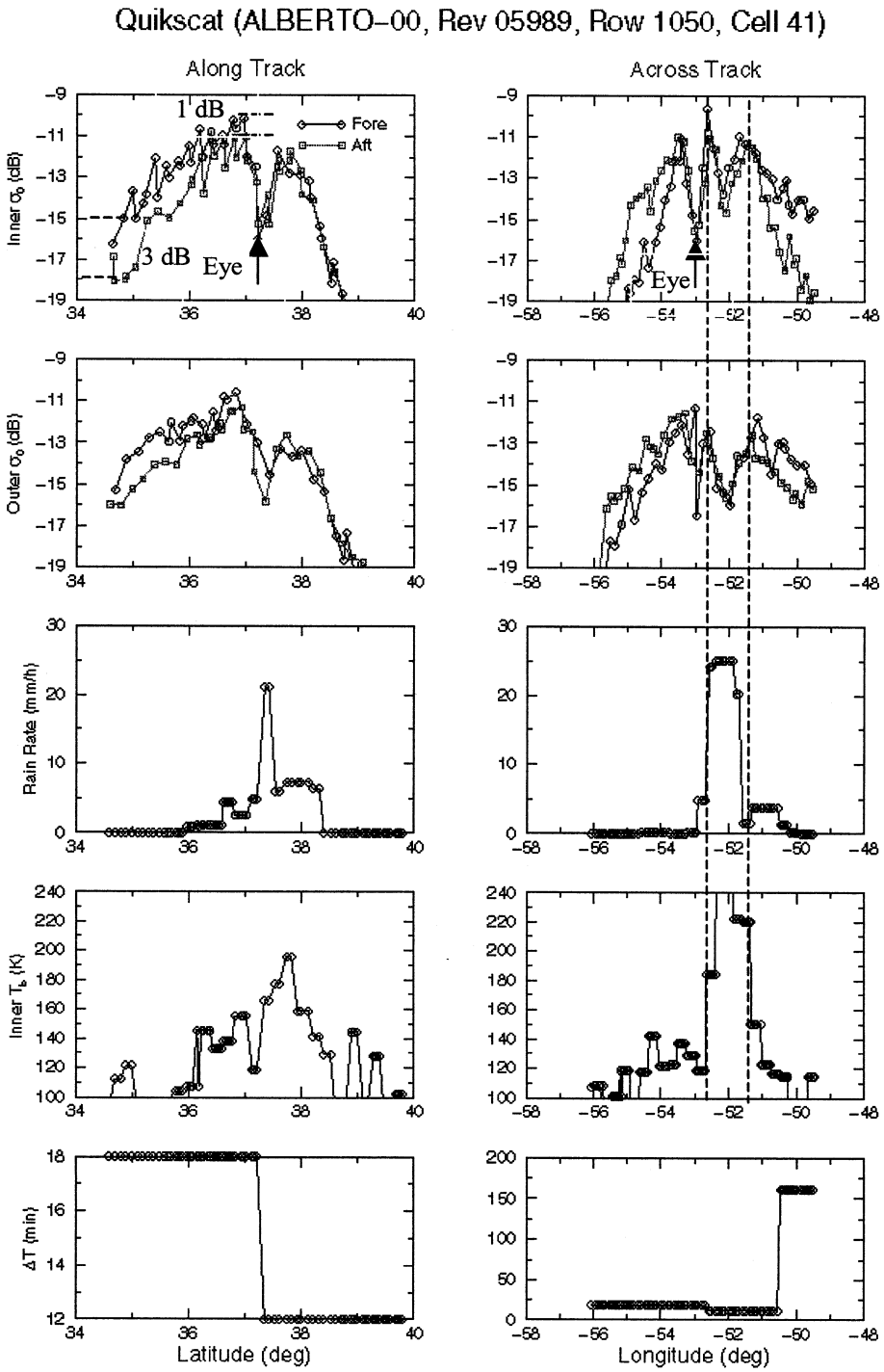

Fig. 3. QuikSCAT $\sigma_0 s$ for hurricane Alberto along and across tracks through the eye of cyclone. The left (right) hand column is for the along (across) track cut of the inner beam $\sigma_0 s$ (first row), outer beam $\sigma_0 s$ (second row), SSM/I rain rate (third row), QuikSCAT brightness temperature (fourth row), and time separation between QuikSCAT and SSM/I observations (fifth row).

rain attenuation factor at an incidence angle of θ is accounted for by the exponential factor. The volume scattering $\sigma_{0\mathrm{RV}}$ (per meter) (m^{-1}) is related to the rain reflectivity factor (Z) [21]

$$\sigma_{0\mathrm{RV}} = 10^{-10}\frac{K_W Z H \pi^5}{\lambda^4}\frac{1-\exp\left(-\frac{2kH}{\cos\theta}\right)}{\frac{2kH}{\cos\theta}} \tag{5}$$

where λ is the radar wavelength in centimeters; H is in meters; and Z has the dimensions of millimeters to the sixth power per cubic meter (mm^6 per m^3). The factor K_W for water varies between 0.89 and 0.93 over 0 °C to 20 °C temperature range and 1–10-cm wavelength range. For simplicity, K_W is set to be 0.9 for our study.

The above radiative transfer equation can be recast into another form

$$\sigma_0 = \sigma_{0R} + A\sigma_{0\mathrm{WIND}} \tag{6}$$

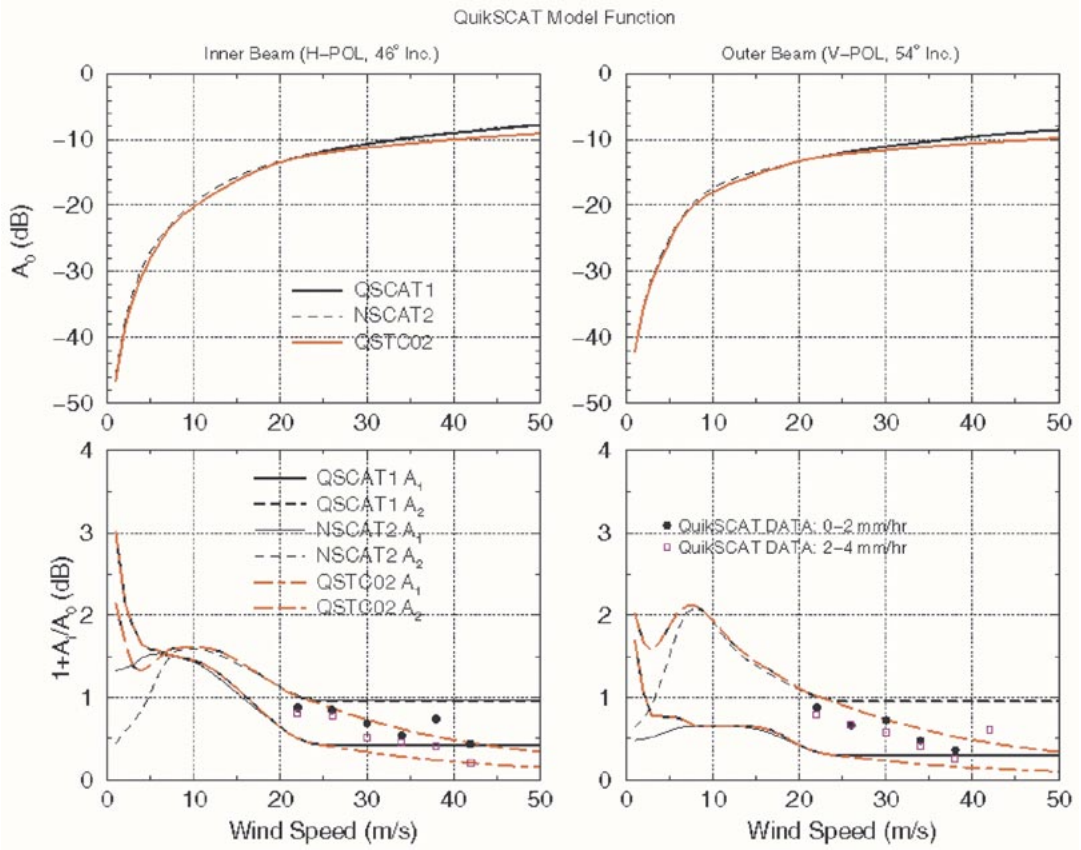

Fig. 4. QuikSCAT A_0, A_1, and A_2 coefficients versus wind speed. QSCAT1 GMF coefficients are labeled by QSCAT1, NSCAT2 GMF by NSCAT2, and revised QSCAT GMF by QSTC02. NSCAT2 GMF has smaller A_1 and A_2 coefficients than those of QSCAT1 GMF at 1–3-m/s wind speeds.

where

$$\sigma_{0R} = \sigma_{0\mathrm{RV}} + A\sigma_{0\mathrm{RS}} \tag{7}$$

$$A = \exp\left(\frac{-2kH}{\cos\theta}\right). \tag{8}$$

In the above equations, σ_{0R} represents the volume scattering from raindrops and attenuated surface scattering from rain-induced surface roughness.

A. HB Model

The dependence of $Z(\mathrm{m}^3)$ and k [in decibels per kilometer (dB/km)] on the rain rate typically takes a power-law form

$$Z = aR^b \tag{9}$$

$$k = \alpha R^\beta. \tag{10}$$

The model coefficients depend on the shape and drop size distribution of raindrops and are modeled by the parameterization developed by Haddad *et al.* [16]. The coefficients are $a = 185.01$, $b = 1.504$, $\alpha = 0.223$, and $\beta = 1.156$, corresponding to the shape parameters "$D = 1.0$" and "$s = 0.38$." The values of these coefficients were derived for 13.8 GHz [16]. We did not rederive these for 13.4 GHz, because our objective is to investigate the sensitivity of wind retrievals to the radiative transfer models. Small changes of modeling coefficients do not affect our general conclusions.

The scattering by the water surfaces roughened by raindrops is typically related to the rain rate by a power law [17]

$$\sigma_{0\mathrm{RS}} = cR^d. \tag{11}$$

Following the model proposed by Bliven *et al.* [17], $d = 0.46$. The proportional coefficient c was determined by matching the model outputs at 1 mm/h with the rain scattering model suggested by [18] (see upper panels of Fig. 5). The results are $c = 0.0063$ for the QuikSCAT inner beam and $c = 0.0050$ for the QuikSCAT outer beam.

We will denote the above radiative transfer model with the modeling coefficients in (9)–(11) from Haddad *et al.* [16] and Bliven *et al.* [17] as the HB model.

B. SY Model

In addition to the HB model, we applied another rain scattering model for the correction of rain effects on wind retrieval. This model was proposed by Stiles and Yueh [18] and hereafter is denoted as the SY model, which was developed based on the analysis of collocated QuikSCAT data, NCEP winds, and SSM/I rain rate. In principle, the SY model is only valid for <20-m/s wind speed and <10-mm/h rain rate conditions because of the limitations of NCEP winds (very few high wind predictions) and SSM/I rain rate. The SSM/I rain rate product cuts off at 25 mm/h, but its range of validity is more limited because the SSM/I 19- and 37-GHz radiometer brightness temperatures are close to saturation for above 10-mm/h rain rate. The use of the SY model for tropical cyclones is an extrapola-

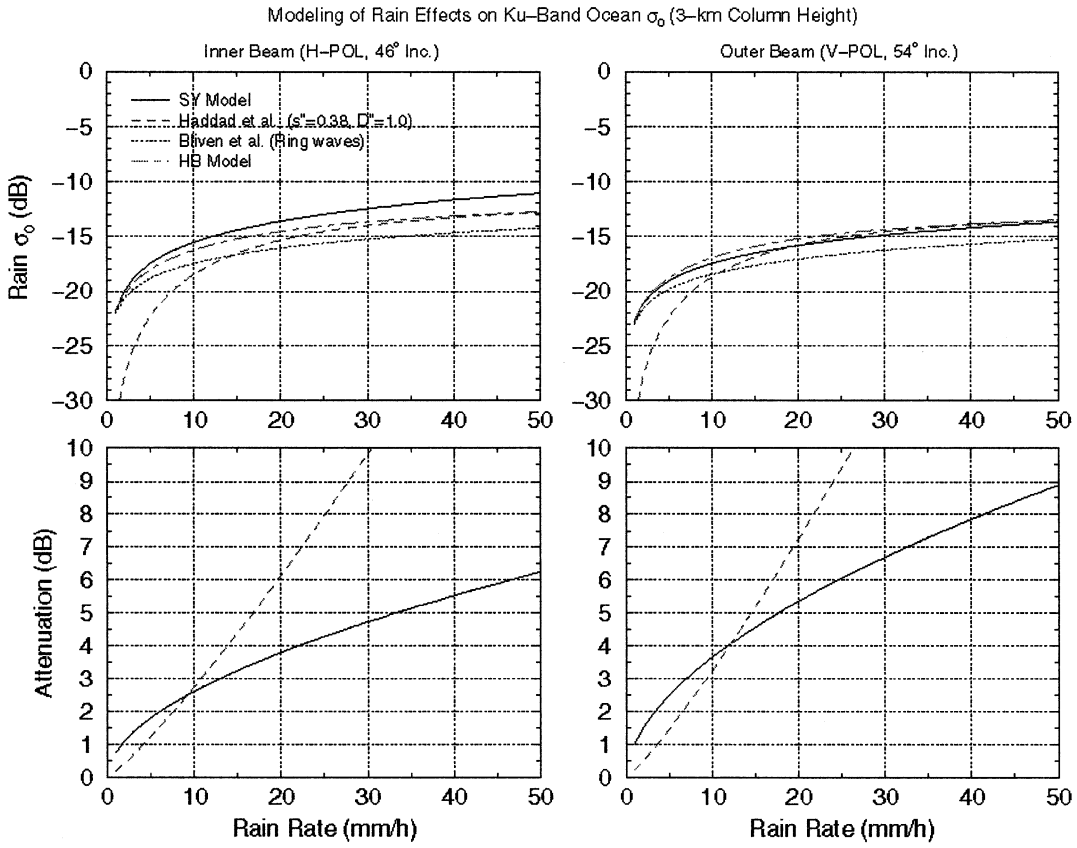

Fig. 5. Illustrations of radiative transfer models for rain published by Stiles and Yueh (SY), Haddad *et al.* for volume scattering and rain attenuation, Bliven *et al.* for ring waves induced by raindrops, and combined Haddad and Bliven's model (HB).

tion. The SY model parameterizes the coefficients σ_{0R} and A by the integrated columnar rain rate RH

$$\sigma_{0R} = f(RH)^g \tag{12}$$

$$A = \exp\left[-p(RH)^q\right]. \tag{13}$$

The unit of H here is in kilometers, instead of meters, which is used for the HB model. The model coefficients are summarized in Table II.

Fig. 5 compares the model predictions of σ_{0R} and A from the HB and SY models for a rain layer with a thickness of 3 km. The modeling elements $\sigma_{0\mathrm{RV}}$ (labeled by Haddad *et al.*) and $\sigma_{0\mathrm{RS}}$ (labeled by Bliven *et al.*), contributing to the HB model, are included for comparison. The upper two panels illustrate the coefficient σ_{0R} for the inner and outer beams. The agreement between SY (solid curve) and HB (short-long dashes) models is reasonable for $<$10 mm/h, but could be different by as much as 2 dB at 50-mm/h rain rate for the inner beam. In the HB model, $\sigma_{0\mathrm{RS}}$ (dotted line) for the scattering by rain-induced surface roughness (e.g., ring waves) is more significant than $\sigma_{0\mathrm{RV}}$, the volume scattering for $<$10-mm/h rain rate, but becomes less significant for $>$15 mm/h.

The major discrepancy between the SY and HB models is the estimates of two-way attenuation, illustrated in the two lower panels of Fig. 5. The HB model predicts a lower attenuation for $<$10-mm/h rain rate, but increases more rapidly for higher rain rates. This could be a result of differences in spatial resolution and the limited accuracy of SSM/I rain rate. The HB model, applied to the precipitation radar with 4–5-km spatial resolution on the Tropical Rain Measuring Mission (TRMM), was derived from the aircraft rain radar data with resolution in the order of kilometers, while the SY model was an empirical analysis of QuikSCAT and SSM/I data with a footprint size in the range of 30–40 km. A large footprint size could result in partial beam filling of rain cells, leading to a more gentle increase of attenuation versus rain rate [14]. Here, we will not attempt to resolve the differences between these two models, but will take advantage of their differences to investigate the response of wind retrievals to rain models.

TABLE II
MODEL COEFFICIENTS OF THE RAIN SCATTERING ATTENUATION MODEL PROPOSED FOR QUIKSCAT [18]

Beam	f	g	p	q
Inner	0.0032	0.64	0.096	0.54
Outer	0.0029	0.54	0.13	0.55

It is known that the top of rain layer in tropics could reach as high as 5 km. However, to obtain unbiased estimates of "surface" rain rate, the monthly climatology used by the SSM/I retrieval algorithm [14] has a rain column height of no more than 3 km in tropics. We presented our analysis for a thickness of 3 km from the perspective of SSM/I retrieval of surface rain rate. Nevertheless, it is important to recognize that the effects of rain on radar backscattering will be more severe for a thinker rain layer.

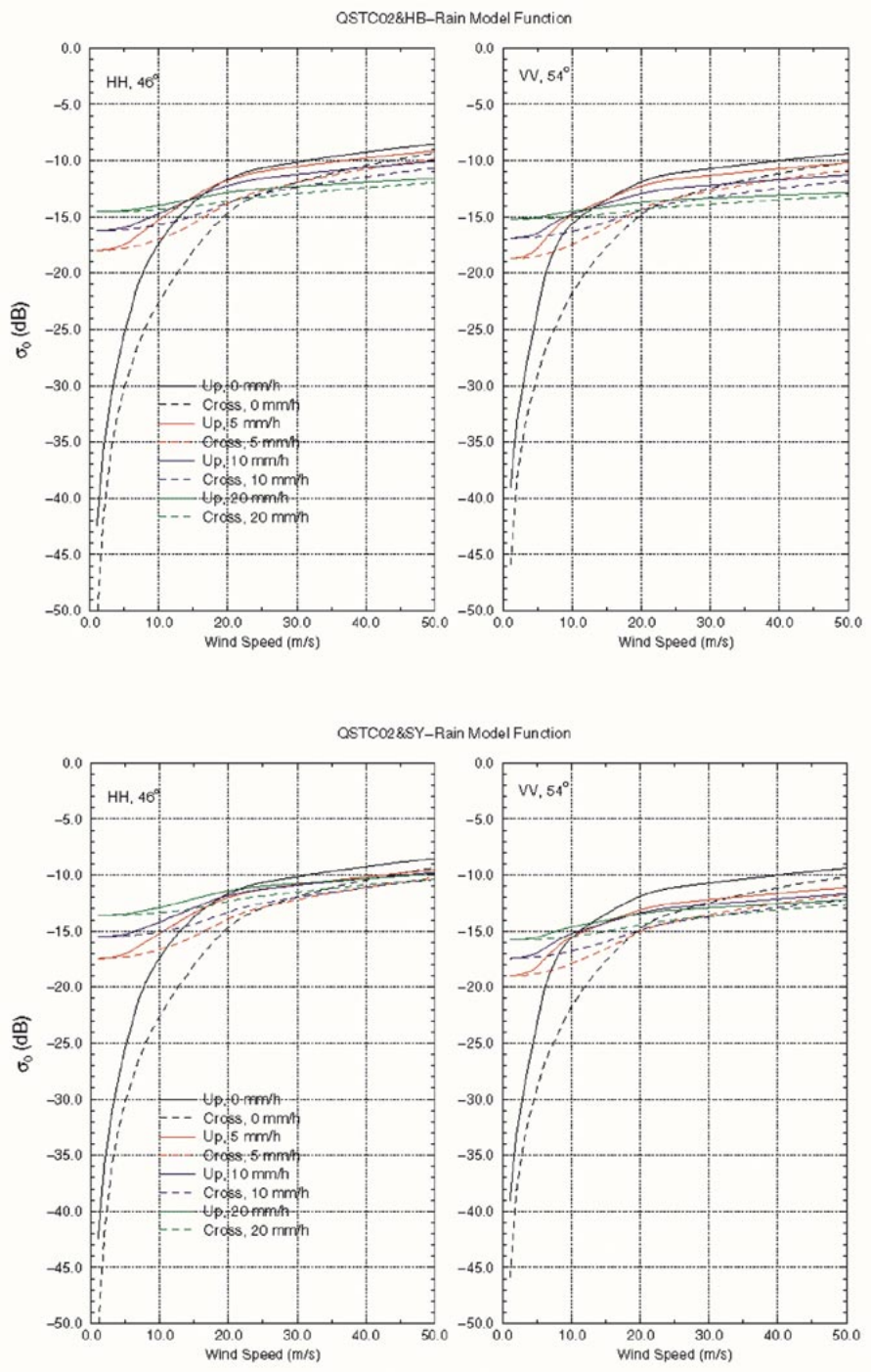

Fig. 6. Model $\sigma_0 s$ versus wind speed for QuikSCAT inner and outer antenna beams. The upper two panels correspond to the HB model, and the lower panels the SY model.

C. Model Characteristics and Comparison

The relative significance of rain and wind on $\sigma_0 s$ depends on the wind speed and rain rate. The total radar $\sigma_0 s$ predicted from the HB and SY models for a rain column height of 3 km are illustrated in Fig. 6. The upwind and crosswind $\sigma_0 s$, indicated by solid and dashed curves, respectively, are plotted to indicate the wind direction dependence of $\sigma_0 s$ under the influence of rain. Each panel includes the model predictions for 0-, 5-, 10-, and 20-mm/h rain rate. The net effects of rain increase $\sigma_0 s$ for light and moderate winds and reduce $\sigma_0 s$ for extreme high winds. Therefore, if uncorrected, rain will result in overestimates of wind speed for light and moderate winds and underestimates for extreme high winds.

Here is an example for more quantitative comparison. The wind-induced surface scattering is about -11 dB for 30-m/s wind speed (upper panels of Fig. 4). A rain rate of 10 mm/h will attenuate the signal by about 2.5 and 3.5 dB for QuikSCAT

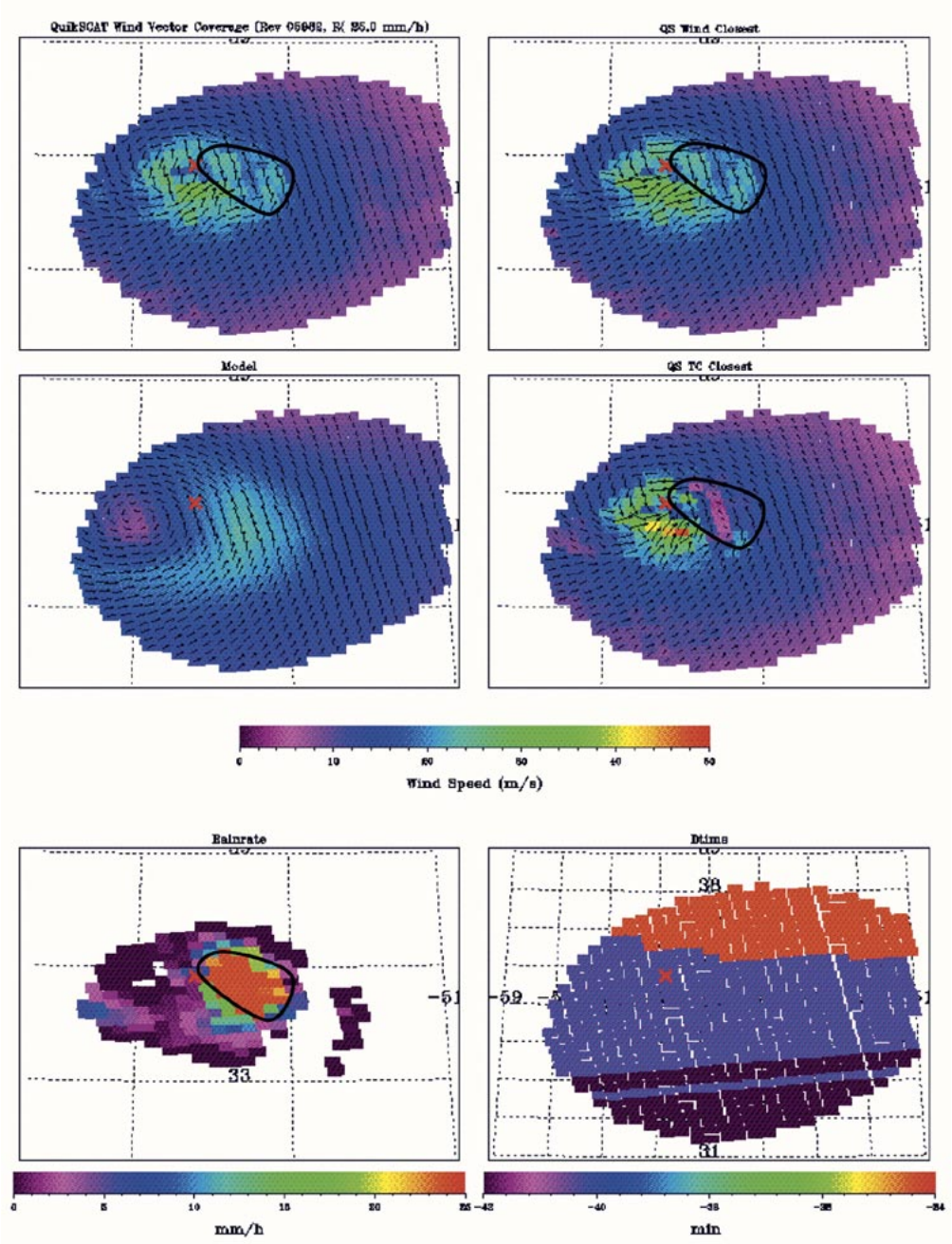

Fig. 7. QuikSCAT winds for hurricane Alberto from rev 5982. The upper left panel plots the wind field of the selected direction ambiguity from the JPL ground data processing system using the QSCAT1 GMF and upper right panel the closest ambiguity field. The NCEP wind is in the middle left panel. The wind field from the retrievals using SY-model is in the middle right panel. The bottom panels are the SSM/I rain rate and time difference from the QuikSCAT observations. The black contour indicates the region of high SSM/I rain rate.

inner and outer beams, respectively (Fig. 5). Hence, the attenuated wind-induced surface scattering $(A\sigma_{0\mathrm{WIND}})$ will be about -13.5 and -14.5 dB. In contrast, the scattering induced by raindrops (σ_{0R}) at 10-mm/h rain rate produces $\sigma_0 s$ of about -16 dB for inner beam and -18 dB for outer beam (upper panels of Fig. 5), which are about 3 dB less than the wind signals. Should the rain rate increase to 15 mm/h, the rain scattering and attenuated wind-induced surface scattering will then be comparable at about -14-dB level for inner beam and -16-dB level for outer beam. The models suggest that the wind-induced signals dominate the rain scattering under the conditions of >30-m/s wind speed and 10-mm/h rain rate for a rain column height of <3 km.

The other effects of rain are to reduce the wind direction sensitivity of $\sigma_0 s$. For light winds (<5 m/s), the rain-induced surface and volume scattering reduces the upwind and crosswind asymmetry of $\sigma_0 s$ to less than 1 dB for heavy rainfall of 10 mm/h (Fig. 6). The reduction of directional dependence is due to the increase in attenuation and rain-induced volume and surface scattering, which are assumed to be independent of wind direction. When the wind speed increases, the wind-induced surface scattering increases and begins to overcome the impact by rain. As the wind speed reaches above a certain threshold, depending on the rain rate and column height, the directional characteristics of wind-induced surface scattering will not be overwhelmed

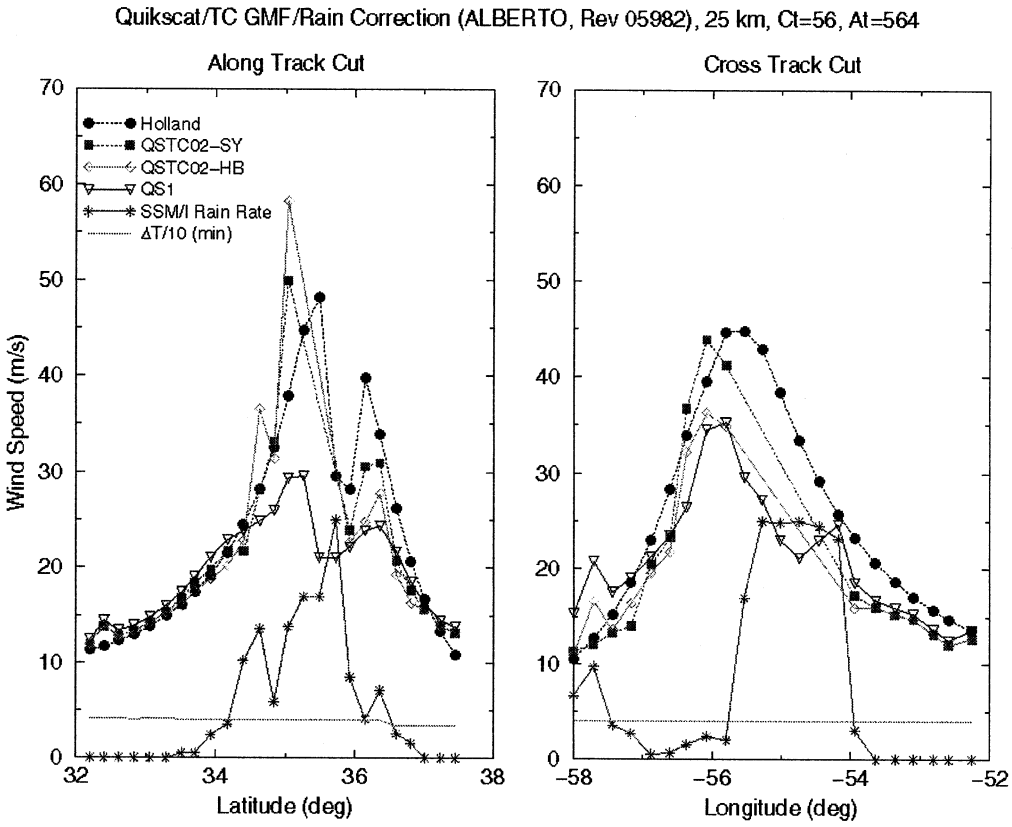

Fig. 8. Wind speed profiles of hurricane Alberto (QuikSCAT rev 5982) along and across track through near the center of cyclone. The JPL ground data processing system output fields are labeled by QS1, wind retrievals using the SY-model by QSTC02-SY, and wind retrievals using the HB-model by QSTC02-HB. The SSM/I rain rate is in millimeters per hour. The time difference (ΔT) between SSM/I and QuikSCAT observations is divided by 10 for illustration.

by rain. For extreme high wind speeds of above 30 m/s, the upwind and crosswind asymmetry of $\sigma_0 s$ do not vary significantly from rain-free to about 10-mm/h conditions.

The major difference between the HB and SY models, as indicated in Fig. 5, is the path attenuation (A) for off 10-mm/h rain rate. This is reflected in Fig. 6 for above 30-m/s wind speed. The estimates of $\sigma_0 s$ from the HB model are about 1 dB higher than that from the SY model at about 5-mm/h rain rate, while the HB model estimates are lower for above 10 mm/h. This implies that the HB model for wind retrievals will result in lower wind speed estimates than the SY model for hurricane force winds at about 5-mm/h rain rate, but will tend to produce higher estimates for above 10-mm/h rain rate.

IV. QuikSCAT Wind Retrievals for Tropical Cyclones

The HB and SY radiative transfer models, together with the revised rain-free GMF (QSTC02), have been applied to the wind retrievals for hurricanes in 1999 and 2000. The differences between the HB and SY models allow the assessment of how the wind retrievals respond to the uncertainties in rain attenuation and scattering models.

The methodology for wind retrieval is described in [12] and is based on the maximum-likelihood measure to minimize the difference between QuikSCAT σ_0 measurements and model estimates under the constraint of SSM/I rain rate. The rain column height is from the monthly climatology maps used to derive the SSM/I rain rate [14]. In general, there are multiple local minima, representing multiple possible solutions (ambiguities) with diverse wind directions. We used the Holland model field [19] to select the closest wind direction ambiguity [12]. The Holland model for the wind fields of tropical cyclones starts with an axially symmetry vortex model and linearly superimposes the forward motion of storm to create an axially asymmetric wind field. This model captures the general characteristics of tropical cyclones [19] and is expected to have a good skill to eliminate the ambiguities with their directions off the true wind direction by more than 90°. However, caution has to be taken for any storms significantly deviating from the Holland model.

The performance of wind retrievals using the SSM/I rain rate is limited by several factors, including the time difference between QuikSCAT and SSM/I passes and difference in spatial resolution. Thus, we limit our retrieval analyses to the cases that the spatial displacement between the SSM/I and QuikSCAT images caused by the motion of storm is less than the size of QuikSCAT WVC, which is 25 km. The other limiting factors for accurate wind retrieval include the accuracy of SSM/I rain rate for above 10 mm/h and the accuracy of radiative transfer models. The SSM/I rain retrievals use the brightness temperatures from 19- and 37-GHz radiometer channels [14], which increase with increasing rain rate, but approach saturation at above 10–15 mm/h. We have to be careful in interpreting the wind retrievals for extreme high SSM/I rain rates. In addition, the RT models for retrievals have neglected the drop size distribution of rain, which plays an important role in predicting the radar scattering by raindrops.

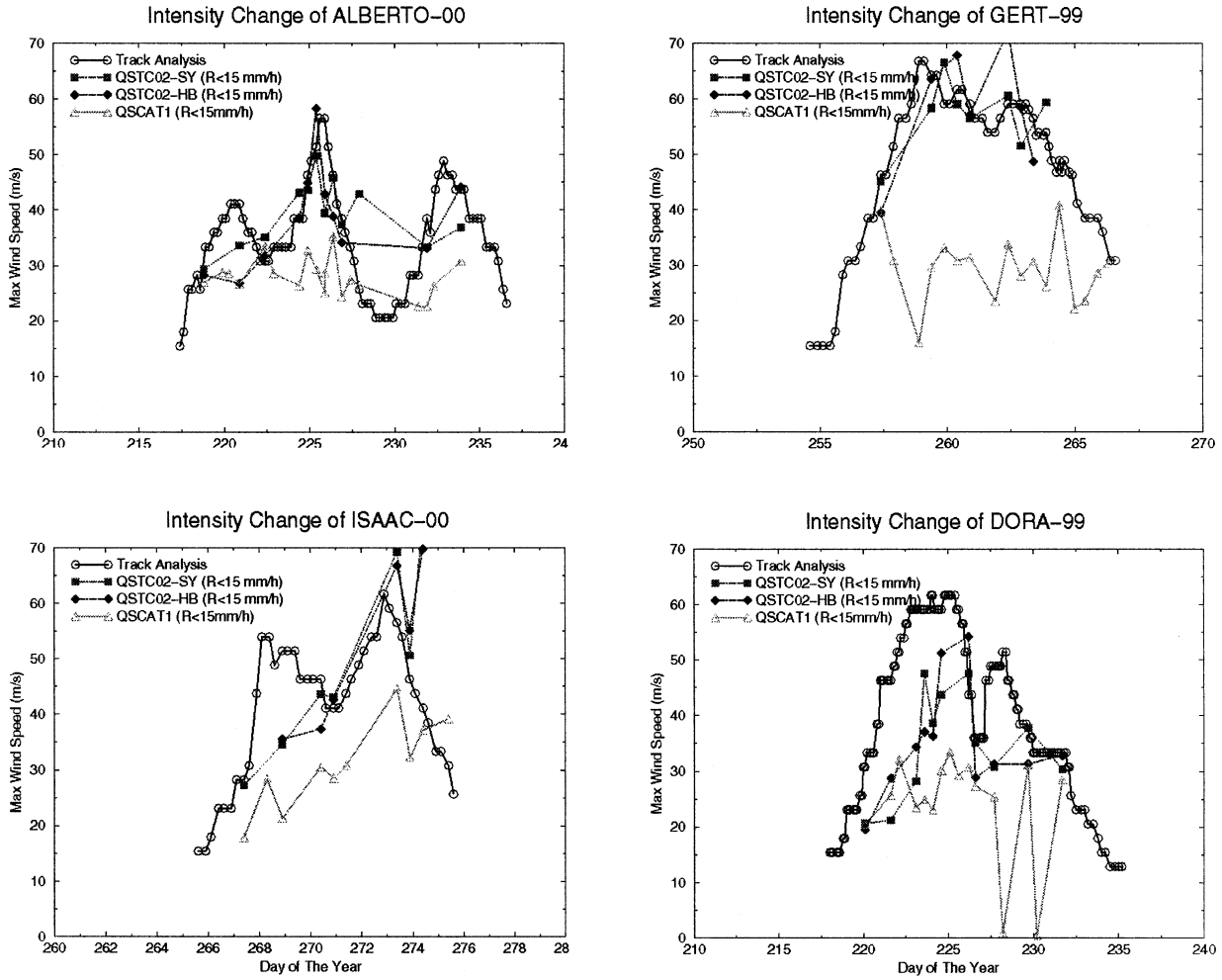

Fig. 9. QuikSCAT estimates of maximum wind speed versus time. (Upper left) Hurricane Alberto in 2000. (Upper right) Hurricane Gert in 1999. (Lower left) Hurricane ISAAC in 2000. (Lower right) Hurricane DORA in 1999.

Fig. 7 illustrates the wind fields for hurricane Alberto retrieved from QuikSCAT rev 5982 data. The middle left panel illustrates the NCEP forecasts, which have a poor representation of the hurricane. The NHC best track analysis indicated that Alberto passed about 300 nautical miles (600 km) east of Bermuda on August 11, 2000 and reached its peak intensity of 110 kn (56 m/s) on the August 12. The best track intensity estimates for Alberto were based on the Dvorak technique [20]. The upper left panel plots the wind field for the selected wind ambiguity from the JPL QuikSCAT ground data processing system, to be denoted as the QS1 product. The QS1 product was retrieved using the QSCAT1 GMF and was not corrected for rain effects. The maximum wind speed in the QS1 product was about 35 m/s, far smaller than the 52-m/s maximum wind speed indicated by the best track analysis (Table I). Part of this underestimate was due to the limited sampling resolution of QuikSCAT with wind retrievals performed on data acquired within a WVC. An estimate of the spatial averaging effect was performed using the Holland model field spatially averaged over 25 km $\times$ 25 km areas with various central pressure (920–970 mbar) and radius of maximum wind (20–40 km). The estimated reduction of maximum wind speed due to the spatial averaging is about 10% to 15%, which cannot account for the large discrepancy between the QS1 maximum wind and the best track analysis. The upper right panel plots the wind speed of the closest wind ambiguities in the QS1 product with respect to the Holland model field, which was generated using the NHC best track analysis and the radius to maximum wind indicated in the QuikSCAT σ_0 data [12]. The closest ambiguity offers small increase of wind speeds for several WVCs to the south of eyewall, but the maximum wind speed remains underestimated. A region to the east of eye by about 100 km has about 15-m/s wind speed (blue color in the figure), lower than that of the neighboring areas and is well coregistered with heavy rain area (orange color in the bottom left panel). The lower-than-expected wind speed estimates are likely due to the rain attenuation effects, which suppress $\sigma_0 s$ for extreme high-wind conditions.

The middle right panel of Fig. 7 plots the wind field retrieved using the SY model and QSTC02 GMF and has indicated stronger wind speeds to the south of eyewall than the QS1 product. However, the wind speeds for the region to the east of eyewall, indicated by high SSM/I rain rate (regions enclosed by black curve in the lower left panel), appear to be underestimated. Similar characteristics have been observed in the wind

retrievals for other revs of QuikSCAT hurricane passes. The results indicate that the SY model performs reasonably well for relatively light rain ($<$10 mm/h), but fails to correct the retrievals for above 15-mm/h SSM/I rain rate.

A quantitative comparison is shown in Fig. 8 for the wind speed retrievals along two cuts near the eye of Alberto: one is along track, and the other is across track. The wind speed retrievals from the QSTC02/SY and QSTC02/HB models reach above 50 m/s, significantly higher than the maximum wind speed estimate of about 35 m/s from the QS1 product. The wind speeds from the regions with $>$15-mm/h rain rate were significant underestimates for the SY model and overestimates for the HB model and were not included in the figure. As a reference, Fig. 8 includes the Holland model field wind averaged over the locations of QuikSCAT σ_0 samples within a WVC. The wind speed retrievals from the SY model seem to have a better agreement with the Holland model field for this case. However, the HB model agrees better with the Holland model for some other hurricanes. The varying performance of the SY and HB models probably reflects the influence of some other variables (e.g., drop size distribution) of rain in tropical storms, in addition to rain rate and column height. Other error sources include the spatial and temporal mismatch between the QuikSCAT and SSM/I observations.

An indicator of the intensity of tropical cyclones is the maximum sustained wind speed. For most hurricanes, the NHC best track analysis performs the maximum wind speed estimates using the Dvorak technique [20], which is based on a pattern matching analysis. QuikSCAT has the potential to augment the best track analysis with independent information regarding the intensity of cyclones and spatial variability of wind field. We performed wind retrievals for several cyclones and searched for the maximum wind speed in the region with less than 15-mm/h rain rate. Because the regions with $>$15 mm/h are excluded, the "maximum" wind speed estimates from QuikSCAT will in general be lower than the maximum wind speed of the storm under consideration. Fig. 9 compares the QuikSCAT estimates with the NHC best track analysis versus time for hurricanes Alberto and Isaac in 2000 and Gert and Dora in 1999. The estimates from QS1 products poorly indicate the strengthening and weakening of cyclones. In contrast, the estimates from the QSTC02 model function with the SY or HB rain model corrections track the intensity changes of Alberto and Gert reasonably well. In particular, the estimates for Gert reach as high as 60 m/s, similar to the best track analysis.

The intensity tracking using the QuikSCAT estimates for Isaac and Dora is not as good, but still indicates the intensification and weakening of cyclones during certain periods of time. It could be that the regions of maximum wind speed for Isaac near day 268 and Dora around days 220–225 were under heavy rain ($>$15 mm/h) and were excluded from the search of maximum wind speed. Nevertheless, the estimates for Dora do reflect the intensity changes near day 225. The results clearly indicate that additional research is needed to improve wind retrievals for certain hurricane conditions.

Due to the temporal and spatial mismatch between SSM/I and QuikSCAT observations, saturation of SSM/I rain retrieval for above 10 mm/h, limited accuracy of the Dvorak technique, the discrepancy between the best track analysis and QuikSCAT estimates for Isaac and Dora remains to be resolved. An improvement from our analysis will require a coincidental, improved rain product and perhaps additional ancillary measurements to estimate the effects of other rain parameters. The data from the SeaWinds scatterometer and Advanced Microwave Scanning Radiometer (AMSR) launched together on the Japanese Advanced Earth Observation Satellite (ADEOS) in December 2002 will offer such an opportunity. AMSR has 6.8- and 10.6-GHz radiometer channels, in addition to the SSM/I frequency channels, and could offer rain rate products valid beyond 20 mm/h.

V. Summary

This paper describes QuikSCAT wind retrievals for tropical cyclones. A direct examination of the QuikSCAT σ_0 data from several intense storms indicates a directional asymmetry of about 0.5–1 dB for wind speeds in the range of 30–50 m/s. The fore- and aft-look differences of $\sigma_0 s$ are used to estimate the amplitude of upwind and crosswind asymmetry (A_2). The A_2 coefficients from the QSCAT1 GMF level off at above 23 m/s, while the A_2 coefficients derived from the data decrease with increasing wind speed and appear to follow the decreasing trend of the QSCAT1 A_2 coefficients at near 20 m/s. The corrections to the QSCAT1 GMF are expressed in a simple analytic form. The evidence on the directional behavior of σ_0 data suggests a potential for wind direction retrievals from spaceborne scatterometers in extreme high-wind events, although an instrument with a better σ_0 detection sensitivity than the QuikSCAT is required.

To compensate for the effects of rain on wind retrieval, two radiative transfer models are examined. The predictions of scattering from raindrops and rain-roughened surfaces agree reasonably well between these two models, but there is a significant difference in the predictions of rain attenuation. Both models are applied to the processing of the QuikSCAT winds and improve the estimates of wind speed for areas with relatively light rain. The results are corroborated with a comparative analysis with the best track intensity estimates of maximum wind speeds for several hurricanes.

However, the results are unsatisfactory for areas of high rain rate ($>$15 mm/h). More detailed studies are recommended to improve the radiative transfer model and rain correction algorithm for wind retrievals. The best data to be available are the coincidental observations from the SeaWinds scatterometer and AMSR launched on December 14, 2002 and should reduce the errors due to temporal and spatial mismatches between QuikSCAT and SSM/I observations. The corrections of other rain parameters, including rain drop size distribution and column height, will need further modeling studies and additional coincidental measurements, such as multifrequency radar and radiometer observations.

Acknowledgment

The authors are grateful to M. Freilich and B. Vanhoff (Oregon State University) and F. Wentz (Remote Sensing Systems) for making the collocated SSM/I products and monthly rain column height maps available for this investigation.

REFERENCES

[1] M. A. Bender, R. J. Ross, R. E. Tuleya, and Y. Kurihara, "Improvements in tropical cyclone track and intensity forecasts using the GFDL initialization system," *Mon. Weather Rev.*, vol. 121, pp. 2046–2061, 1993.

[2] S. Dickinson and R. A. Brown, "A study of near-surface winds in marine cyclones using multiple satellite sensors," *J. Appl. Meteorol.*, vol. 35, pp. 769–781, June 1996.

[3] C. S. Hsu, W. T. Liu, and M. G. Wurtele, "Impact of scatterometer winds on hydrologic forcing and convective heating through surface divergence," *Mon. Weather Rev.*, vol. 125, no. 7, pp. 1556–1576, July 1997.

[4] W. T. Liu, H. Hu, and S. Yueh, "Quikscat and TRMM reveal the interplay between dynamic and hydrologic parameters in Hurricane Floyd," *EOS Trans.*, vol. 81, no. 23, pp. 253–257, June 6, 2000.

[5] R. A. Brown, Ed., "Remote sensing of the Pacific Ocean by satellites," in *Global High Wind Deficiency*. Marrickville, Australia: Southwood, 1998.

[6] M. A. Bourassa, D. M. Legler, J. J. O'Brien, and S. R. Smith, "SeaWinds validation with research vessels," *J. Geophys. Res.*, vol. 108, no. C2, Feb. 2003.

[7] L. Zeng and R. Brown, "Scatterometer observations at high wind speeds," *J. Appl. Meteorol.*, vol. 37, pp. 1412–1420, 1998.

[8] W. L. Jones, V. J. Cardone, W. J. Pierson, J. Zec, L. P. Price, A. Cox, and W. B. Sylvester, "NSCAT high-resolution surface wind measurements in typhoon violet," *J. Geophys. Res.*, vol. 104, pp. 11 247–11 259, 1999.

[9] J. Carswell, S. C. Carson, R. E. McIntosh, F. K. Li, G. Neumann, D. J. Mclaughlin, J. C. Wilkerson, P. G. Black, and S. V. Nghiem, "Airborne scatterometers: Investigating ocean backscatter under low- and high-wind conditions," *Proc. IEEE*, vol. 82, pp. 1835–1860, Dec. 1994.

[10] W. J. Donneley, J. R. Carswell, R. E. McIntosh, P. S. Chang, J. Wilkerson, F. Marks, and P. G. Black, "Revised ocean backscatter models at C and Ku-band under high wind conditions," *J. Geophys. Res.*, vol. 104, pp. 11 485–11 497, 1999.

[11] S. H. Yueh, R. West, F. Li, W.-Y. Tsai, and R. Lay, "Dual-polarized Ku-band backscatter signatures of hurricane ocean winds," *IEEE Trans. Geosci. Remote Sens.*, vol. 38, pp. 73–88, Jan. 2000.

[12] S. H. Yueh, B. W. Stiles, W.-Y. Tsai, H. Hu, and W. T. Liu, "QuikSCAT geophysical model function for tropical cyclones and applications to Hurricane Floyd," *IEEE Trans. Geosci. Remote Sensing*, vol. 39, pp. 2601–2612, Dec. 2001.

[13] W. L. Jones, K. Ahmad, J. D. Park, and J. Zec, "Validation of QuikSCAT radiometer rain rates using the TRMM microwave radiometer and the special sensor microwave imager," in *Proc. IGARSS*, Toronto, ON, Canada, June 24–28, 2002.

[14] F. J. Wentz and R. W. Spencer, "SSM/I rain retrievals within a unified all-weather ocean algorithm," *J. Atmos. Sci.*, vol. 55, no. 6, pp. 1613–1627, 1998.

[15] F. J. Wentz, M. H. Freilich, and D. K. Smith, "NSCAT-2 geophysical model function," in *Proc. Fall AGU Meeting*, San Francisco, CA, 1998.

[16] Z. S. Haddad, D. A. Short, S. L. Durden, E. Im, S. Hensley, M. Grable, and R. A. Black, "A new parameterization of the rain drop size distribution," *IEEE Trans. Geosci. Remote Sensing*, vol. 35, pp. 532–539, May 1997.

[17] L. F. Bliven, P. W. Sobieski, and C. Craeye, "Rain generated ring-waves: Measurements and modeling for remote sensing," *Int. J. Remote Sens.*, vol. 18, no. 1, pp. 221–228, 1997.

[18] B. Stiles and S. Yueh, "Impact of rain on wind scatterometer data," *IEEE Trans. Geosci. Remote Sensing*, vol. 40, pp. 1973–1983, Sept. 2002.

[19] G. Holland, "An analytic model of the wind and pressure profiles in hurricanes," *Mon. Weather Rev.*, vol. 108, pp. 1212–1218, 1980.

[20] V. F. Dvorak, "Tropical cyclone intensity analysis and forecasting from satellite imagery," *Mon. Weather Rev.*, vol. 103, pp. 420–430, 1975.

[21] F. T. Ulaby, R. K. Moore, and A. K. Fung, *Microwave Remote Sensing: Active and Passive*. Norwood, MA: Artech House, 1981, vol. 1, p. 315.

Simon H. Yueh (M'92–SM'01) received the Ph.D. degree in electrical engineering in 1991 from the Massachusetts Institute of Technology (MIT), Cambridge, in 1991.

He was a Postdoctoral Research Associate at MIT from February to August 1991. In 1991, he joined the Radar Science and Engineering Section, Jet Propulsion Laboratory (JPL), Pasadena, CA, and worked as a Radar System Engineer for the SIR-C, NSCAT, and SeaWinds missions. He is the supervisor of a radar system engineering and algorithm development group and is a Principal Engineer at JPL. He led the Aquarius instrument team for a successful National Aeronautics and Space Administration (NASA) Earth System Science Pathfinder mission proposal. He has been the Principal/Co-Investigator of numerous research projects, including the polarimetric wind radiometer research, the NUSCAT project for hurricane wind measurements, the Passive/Active L-/S-band (PALS) radiometer and radar project, the NASA Instrument Incubator Project for a mission concept using a large mesh-deployable antenna for soil moisture and ocean salinity sensing, the airborne polarimetric radar (POLSCAT) for ocean wind velocity measurements, the POLSCAT/Cold Land Process Experiment in 2002-2003, and the Advanced Component Technology lightweight dual-frequency antenna feed project. He is leading the development of the Cold Land Process Pathfinder mission concept at JPL. He also serves on the NASA Independent Assessment Team for the Global Precipitation Mission, Cold Land Process Working Group, Salinity Sea Ice Working Group, Ocean Vector Wind Science Team, and WINDSAT Science Team. He has authored four book chapters and published 46 refereed articles and more than 100 conference presentations. His current fields of interest include techniques and instrument developments for microwave remote sensing of soil moisture, ocean surface salinity, ocean winds and polar ice, and theories for active and passive microwave remote sensing. He is an Associate Editor of *Radio Science.*

Dr. Yueh received the IEEE GRSS Transactions Prize Paper Award in 1995, the JPL Lew Allen Award in 1998, the IEEE IGARSS 2000 Best Paper Award, the JPL Ed Stone Award in 2002, and IEEE GRSS Transaction Prize Paper Award in 2002. He is a member of the American Geophysical Union.

Bryan W. Stiles received the B.S. degree in electrical engineering from the University of Tennessee, Knoxville, in 1992 and the Ph.D. degree from the University of Texas, Austin in 1997. His doctoral dissertation work proved the universal approximation capability of certain dynamic artificial neural networks.

He is currently with the Jet Propulsion Laboratory (JPL), Pasadena, CA, developing SAR, scatterometer, radiometer, and altimeter ground processing algorithms for the onboard radar on the Cassini mission to Saturn. In June 1997, he became a member of the technical staff at the JPL, where he has simulated the behavior of spaceborne scatterometers (NSCAT and SeaWinds) as well as analyzed the data returned from these instruments. He is interested in statistical techniques for determining and visualizing relationships between remote sensor data and geophysical phenomena.

W. Timothy Liu received the Ph.D. degree in atmospheric sciences from the University of Washington, Seattle, in 1978.

He is currently a Principal Scientist at the Jet Propulsion Laboratory (JPL), California Institute of Technology, Pasadena. He has been a Principal Investigator on studies concerning ocean–atmosphere interaction and satellite oceanography since he joined JPL in 1979. He has been the Leader of the Air–Sea Interaction and Climate Team, supervising a team of meteorologists and oceanographers in their scientific researches since 1989. He has been the Project Scientist of a series of NASA scatterometer missions—NSCAT, QuikSCAT, and SeaWinds. He became a Senior Research Scientist at JPL, which is equivalent to a Full Professor in major U.S. universities, in 1993.

Dr. Liu is a Fellow of the American Meteorological Society. He received the Distinguished Science Award of the Pan Oceanic Remote Sensing Award Committee in 2002. In 1996, he received an Honor Professorship at China Ocean University. He received the NASA Medal for Exceptional Scientific Achievement for his pioneering work in ocean surface heat flux in 1990 and the NASA Exceptional Achievement Medal in leading the NSCAT Science Team in air–sea interaction studies in 1998. He has served on numerous science working groups and advisory panels of NASA, including the Advisory Committee of the NASA Earth Science Division. He was a member of various working groups of the World Climate Research Program and has participated in the design and implementation of field campaigns. He has served on the editorial boards of several scientific journals.